Electronic Supplementary Material (ESI) for Physical Chemistry Chemical Physics.

Supplementary information

Defect passivation induced strong photoluminescence enhancement of rhombic monolayer MoS_2

Weitao Su[1,*], Long Jin[1], Xiaodan Qu[1], Dexuan Huo[1,*], Li Yang[2]

[1]Institute of Materials Physics, Hangzhou Dianzi University, 310018, Hangzhou, China

[2] Department of Chemistry, Xi'an Jiaotong-Liverpool University, 215123, Suzhou, China

Corresponding author: Weitao Su, suweitao@hdu.edu.cn;

DexuanHuo, dxhuo@hdu.edu.cn

Telephone & Fax: +86-571-86878539

§1 Mapping of a triangular monolayer

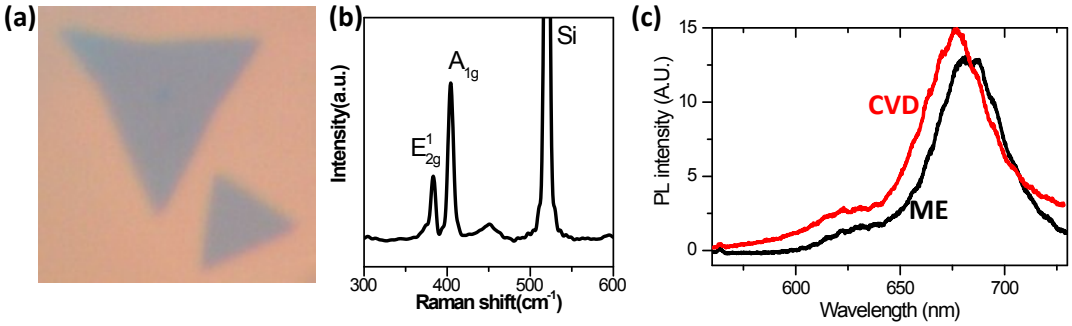

Figure S1. (a) Optical image of triangular monolayer MoS_2; (b), Raman spectrum of this triangular plate; (c), PL intensity of monolayer in (a) in comparison to mechanically exfoliated monolayer.

§2 AFM of flakes with different colour

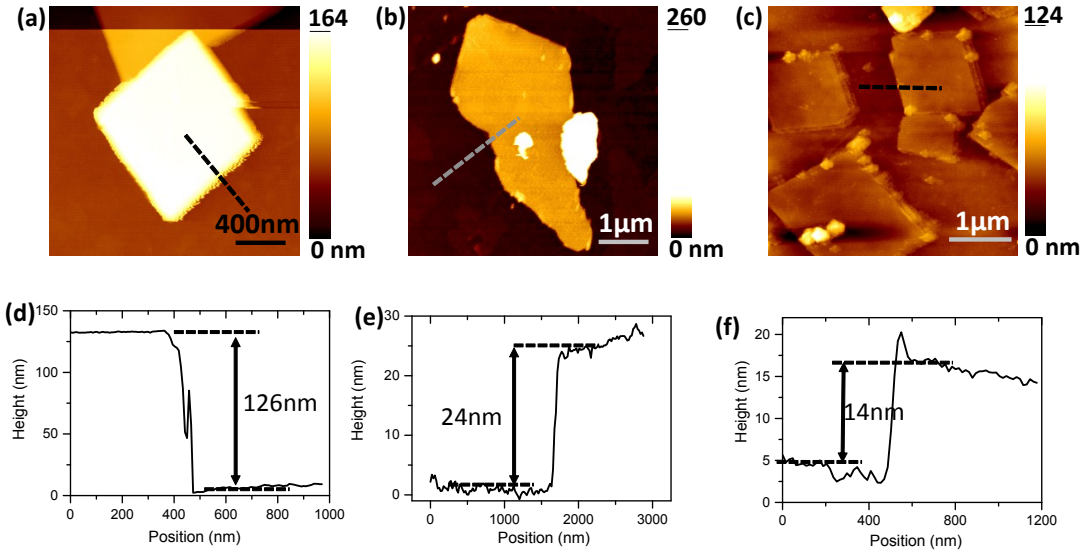

Figure. S2, (a), (b) and (c): AFM topographic images of yellow, grey and another violet flake, respectively; (d), (e) and (f), line profile at corresponding position of (a)-(c), respectively.

§3 Fitting of the PL spectra using four exciton model

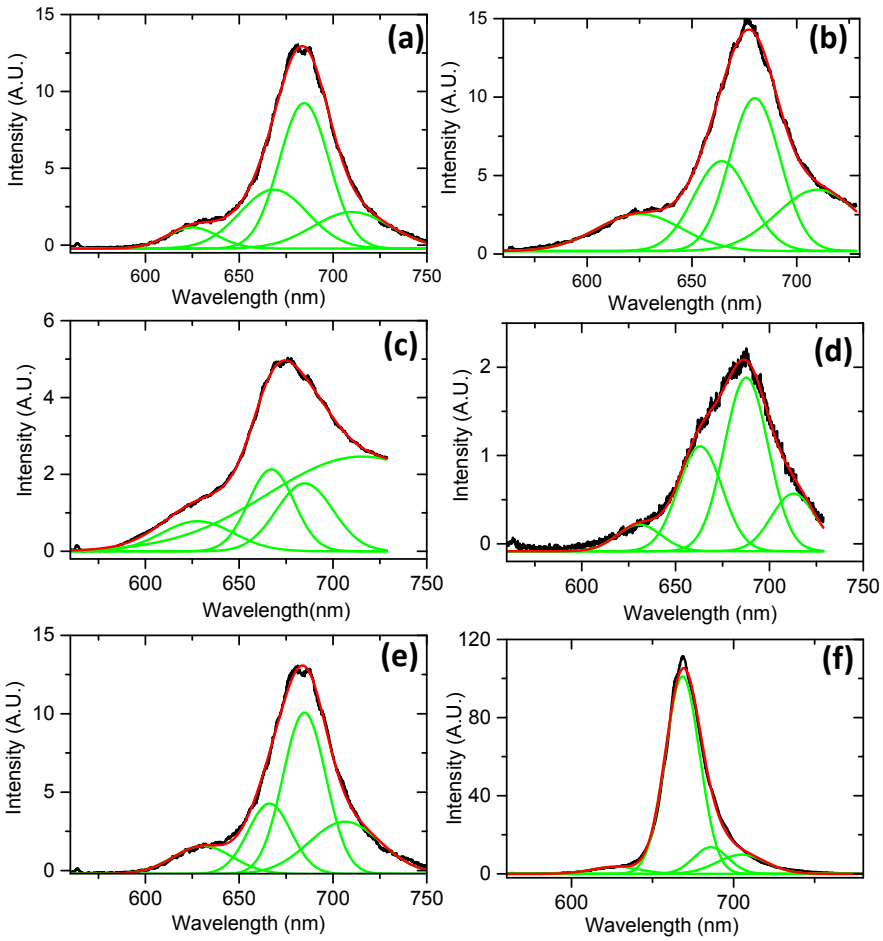

Figure. S3, PL fitting of different samples: (a) ME monolayer; (b)CVD triangular MoS_2; (c) R1; (d) R2; (e) R3; (f) R4.

§4 Normalized PL and D exciton analysis

Normalized PL spectra of mechanically exfoliated monolayer (ME), CVD grown triangular monolayer (CVD) and rhombic monolayer on MoO_2(R4) are shown in Figure S4(a). The peak position of B exciton(B), neutral exciton (A^0), trion (A^-)and D exciton(D) are marked at the position of dashed lines. It can be found that both the ME and CVD monolayer MoS_2 samples have much higher D exciton intensity than rhombic monolayer MoS_2. Figure S4 (b) shows the intensity ratio of D exciton, I_D/I_{sum}, of the three samples, where $I_{sum} = I_B + I_{A^0} + I_{A^-} + I_D$ is the summarized PL intensity of all the excitons. I_B, I_{A^0}, I_{A^-} and I_D are PL intensities of B, neutral exciton, trion and D excitons, respectively. It can be found that I_D/I_{sum} ratio of rhombic monolayer on MoO_2 is only 40% of that of ME and CVD monolayer MoS_2, which indicates much low density of defects on rhombic monolayer MoS_2.

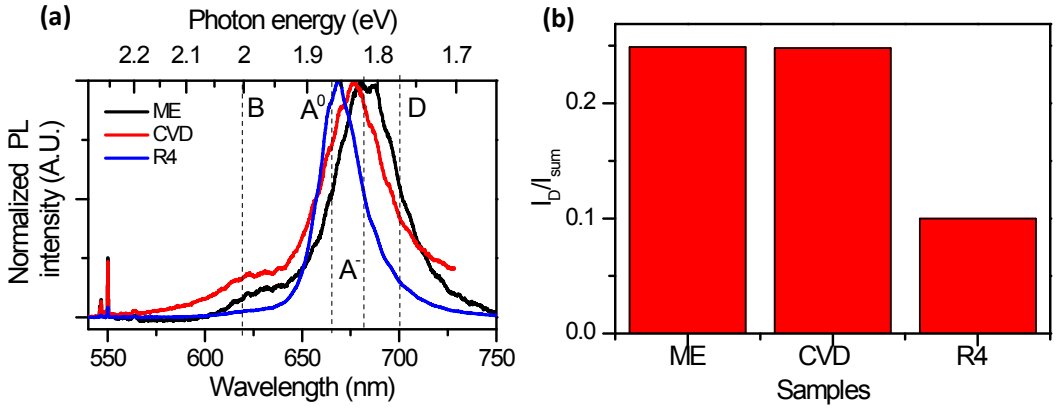

Figure S4 (a) Normalized PL spectra of pristine monolayer MoS_2 prepared by mechanical exfoliation (ME), CVD grown triangular monolayer (CVD) and rhombic monolayer on MoO_2(R4); (b) the intensity ratio of D exciton*(I_D)* in the summarized PL intensity of all the excitons ($I_{sum}=I_B+I_{A0}+I_{A^-}+I_D$)

§5 Supercell structure of pristine MoS_2

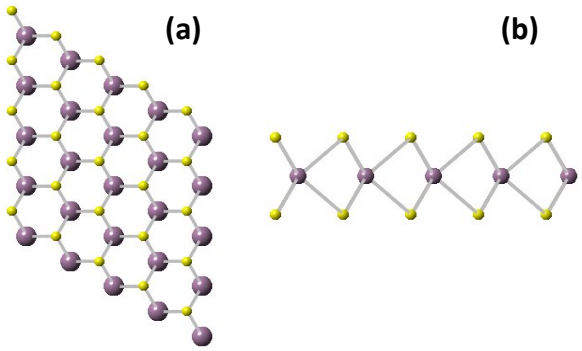

Figure. S5, Supercell of pristine MoS_2: (a) top view; (b) side view.

In DFT calculation, PBE potential was used in companion with spin-orbit coupling. Constant value of $K_{max}\times R_{MT}=7.0$ was maintained throughout our calculations, which controls the size of the basis sets in calculations. The convergence criteria for charge and energy were set to be 1 $\times 10^{-4}$eV and 1 $\times 10^{-4}$ Ry during self-consistency cycles, respectively. The geometric optimization is carried out at different compression ratios. The lattice parameters are calculated at the lowest energy. Figure S6 (a) shows the energy convergence of geometric optimization of pristine monolayer MoS_2 (curve 1), monolayer MoS_2 with a sulphur vacancy(curve 2) and monolayer MoS_2 with vacancy passivated by oxygen atom(curve 3). It can be found that the monolayer MoS_2 with sulphur vacancy passivated by an oxygen atom has the lowest energy, which indicates

the most stable state. Figure S6(b) shows the energy convergence of MoS_2 samples during the self-consistency cycles, energy convergence with number of iteration. After the first six iterations, the energies increase slightly to the stable energies where energy convergence <1 $\times 10^{-4}$ Ry. The number of iteration of pristine monolayer MoS_2 (curve 1) is 16, monolayer MoS_2 with a sulphur vacancy(curve 2) is 22 and monolayer MoS_2 with vacancy passivated by oxygen atom(curve 3) is 24.

Mo DOS and S DOS in figure 4(d), (f) and (h) are summarized DOS of all the Mo atoms and S atoms, respectively. The DOS of oxygen atoms in Figure 4(f) is the DOS of oxygen atom introduced.

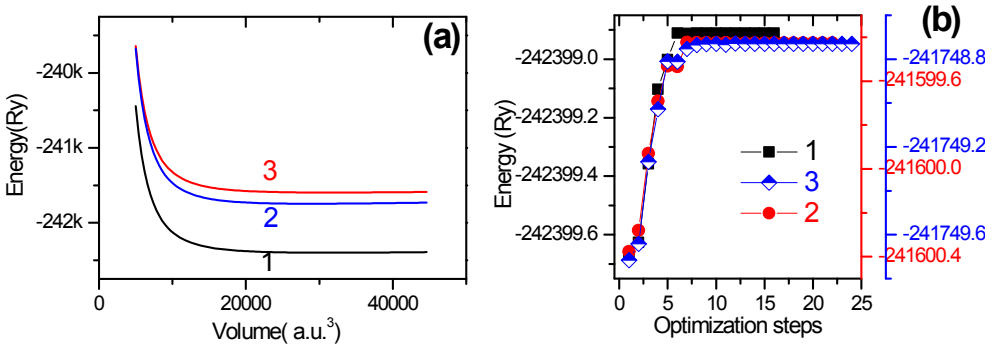

Figure S6 (a), Energy convergence of geometric optimization of pristine monolayer MoS_2 (curve 1), monolayer MoS_2 with a sulphur vacancy (curve 2) and monolayer MoS_2 with vacancy passivated by oxygen atom (curve 3) ;(b), Energy convergence of MoS_2 samples with optimization steps.

§6 exciton dynamics with presence of trapping state

The defect passivation effect can be understood by exciton dynamics with a trapping state schematically shown in Figure.S7(a). In Figure.S7(a), neutral exciton has four possible transition processes : (1) transition to ground state via radiative recombination process with decay rate of Γ_{A^0} ;(2)transition to ground state via carrier-phonon scattering & Auger process with decay rate of $k_{i\_A^0}$; (3) transition to trion state with decay rate of k_{A^-} ; (4), bound to deep trap state caused by sulphur vacancy with decay rate of $k_{D_{A^0}}$.

Trion has three possible transition processes: (1) transition to ground state via radiative recombination process with decay rate of Γ_{A^-}; (2)transition to ground state via carrier-phonon scattering & Auger process with decay rate of $k_{i\_A^-}$; (3) bound to deep trap state caused by sulphur vacancy with decay rate of $k_{D_{A^-}}$.

Once trion or neutral exciton are bound with traps, they become trapped excitons and have two possible transition processes : (1) transition to ground state via radiative recombination process with decay rate of Γ_D; (2) transition to ground state via carrier-phonon scattering & Auger process with decay rate of k_{i_D}

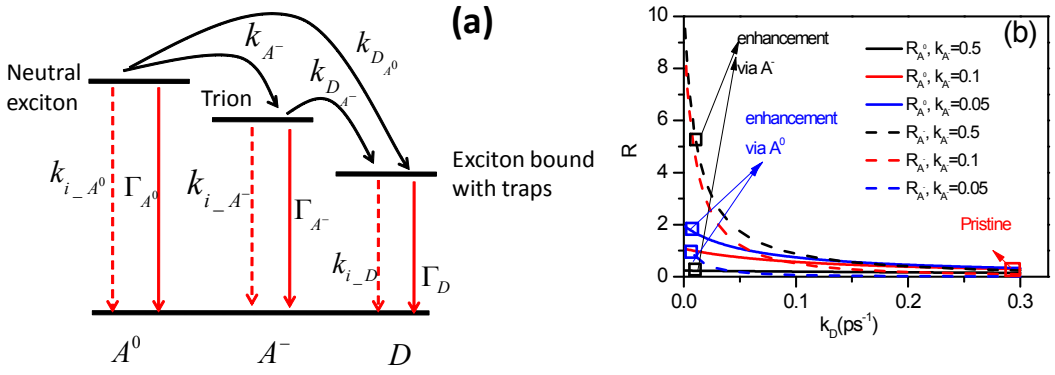

Figure. S7 (a) Exciton dynamics in monolayer MoS_2; (b) Calculated different quantum yield at different k_D.

The exciton dynamic equations at different states can be deduced from exciton model proposed by Mouri *et al*. [1] and Su et al[2] as following:

$$\frac{dN_{A^0}}{dt} = G - \left(\Gamma_{A^0} + k_{A^-} + k_{D_{A^0}} + k_{i\_A^0}\right)N_{A^0} \quad \text{(S1)}$$

$$\frac{dN_{A^-}}{dt} = k_{A^-}N_{A^0} - \left(\Gamma_{A^-} + k_{D_{A^-}} + k_{i\_A^-}\right)N_{A^-} \quad \text{(S2)}$$

$$\frac{dN_D}{dt} = k_{D_{A^0}} N_{A^0} + k_{D_{A^-}} N_{A^-} - (\Gamma_D + k_{i\_D}) N_D \quad \text{(S3)}$$

Where G is generation rate of neutral exctions; N_{A^0}, N_{A^-} and N_D are the population of neutral, charged and trapped exactions at trapping state, respectively .

In the steady case, the exponent items of the solution of eq. S1-S3 vanish. The population of excitons at different states can be deduced from eq.S1 to eq.S3 as

$$N_{A^0} = \frac{G}{\Gamma_{A^0} + k_{A^-} + k_{D_{A^0}} + k_{i\_A^0}} \quad \text{(S4)}$$

$$N_{A^-} = \frac{k_{A^-}}{\Gamma_{A^-} + k_{D_{A^-}} + k_{i\_A^-}} N_{A^0} \; x = \frac{k_{A^-}}{\Gamma_{A^-} + k_{D_{A^-}} + k_{i\_A^-}} \quad \text{(S5)}$$

$$N_D = \frac{k_{D_{A^0}} + x k_{D_{A^-}}}{\Gamma_D + k_{i\_D}} N_{A^0} \quad \text{(S6)}$$

The observed intensities of A^0 , A^- excitons and exciton bound to traps are expressed as

$$I_{A^0} = R_{A^0} G \quad \text{(S7)}$$

$$I_{A^-} = R_{A^-} G \quad \text{(S8)}$$

$$I_D = \frac{\gamma_D (k_{D_{A^0}} + x k_{D_{A^-}})}{\Gamma_D} N_{A^0} \quad \text{(S9)}$$

Where R_{A0} and R_{A^-} denote the quantum yield of netural exciton and trion,respectively, and can be expressed as

$$R_{A^0} = \frac{\Gamma_{A^0}}{\Gamma_{A^0} + k_{A^-} + k_{D_{A^0}} + k_{i\_A^0}} \quad \text{(S10)}$$

$$R_{A^-} = \frac{k_{A^-}\Gamma_{A^-}}{(\Gamma_{A^-} + k_{D_{A^-}} + k_{i\_A^-})(\Gamma_{A^0} + k_{A^-} + k_{D_{A^0}} + k_{i\_A^0})} \quad \text{(S11)}$$

In order to simplify the discussion, we set $k_{D_{A^0}} = k_{D_{A^-}} = k_D$. In pristine monolayer MoS_2 where deep trapping energy levels presence, k_D is usually larger than 0.3ps^{-1}. As shown by Figure.S7(b), the quantum yield of neutral exciton and trion of pristine MoS_2 are lower than 0.3%. This also indicates that most of the free excitons(neutral exciton and trion) are trapped to the trapping states and transit to ground state via non-radiative recombination. With sulphur vacancies passivated by oxygen atoms, the trapping states disappear and k_D is greatly reduced to be lower than 0.01ps^{-1}. Consequently, the quantum yield of neutral exciton and trion are greatly enhanced by tens of times(Figure.S7(b)). If k_{A^-} is smaller than 0.05ps^{-1}, the enhanced PL intensity of neutral exciton is much stronger than that of trion, which corresponds to the enhanced PL intensity of sample R4 in Figure.3(a) of the main text.